ELSEVIER

Polymer 44 (2003) 2537–2545

polymer

www.elsevier.com/locate/polymer

Melting behaviors, isothermal and non-isothermal crystallization kinetics of nylon 1212

Minying Liu[a], Qingxiang Zhao[a,*], Yudong Wang[a], Chenggui Zhang[a], Zhishen Mo[b], Shaokui Cao[a]

[a]*College of Materials Engineering, Zhengzhou University, Zhengzhou 450052, People's Republic of China*
[b]*State Key Laboratory of Polymer Physics and Chemistry, Changchun Institute of Applied Chemistry, Chinese Academy of Sciences, Changchun 130022, People's Republic of China*

Received 31 July 2002; received in revised form 24 December 2002; accepted 16 January 2003

Abstract

Isothermal crystallization, subsequent melting behavior and non-isothermal crystallization of nylon 1212 samples have been investigated in the temperature range of 160–171 °C using a differential scanning calorimeter (DSC). Subsequent DSC scans of isothermally crystallized samples exhibited three melting endotherms. The commonly used Avrami equation and that modified by Jeziorny were used, respectively, to fit the primary stage of isothermal and non-isothermal crystallizations of nylon 1212. The Avrami exponent n was evaluated, and was found to be in the range of 1.56–2.03 for isothermal crystallization, and of 2.38–3.05 for non-isothermal crystallization. The activation energies (ΔE) were determined to be 284.5 KJ/mol and 102.63 KJ/mol, respectively, for the isothermal and non-isothermal crystallization processes by the Arrhenius' and the Kissinger's methods.

Keywords: Nylon 1212; Crystallization; Differential scanning calorimeter

1. Introduction

Linear aliphatic polyamides, commonly known as nylons, occupy a prominent position in the realm of polymers. Nylons are semi-crystalline polymers that usually exhibit a relatively high modulus, toughness and strength, low creep and good temperature resistance that allow wide spread use of this family of polymers as fibers and engineering thermoplastics [1,2]. Since their discovery by Carothers in 1934 [3,4], many nylons have been investigated, a number of which have been commercialized during the past 50 years [2]. But relatively little effort has been made to explore and investigate nylons that comprise longer alkane segments (≥deodecane). The most important attributes of these polyamides are superb toughness, high tensile strength, abrasion resistance, dimensional stability, superb wet strength retention, and low tissue reaction [5–7]. Long alkane segments nylons such as nylon 12 have been widely used in military, machinery, electron equipment, automobile, information and aviation industries [8–11].

A literature review yields several reports that describe AABB nylons that comprise long aliphatic segments [12–16]. But the literature on poly(dodecamethylene dodecanoamide), which is called nylon 1212, is very few. Jones NA et al. [17,18] have studied the structure of a series of even–even nylons. According to Jones NA's study, in room temperature, nylon 1212 exhibits both the α_p and β_p structures. Unite cell dimensions are as follows: α_p structures a = 0.490 nm, b = 0.521 nm, c = 3.23 nm, $\alpha = 50°$, $\beta = 77°$, and $\gamma = 64°$; β_p structures a = 0.490 nm, b = 0.802 nm, c = 3.23 nm, $\alpha = 90°$, $\beta = 77°$, $\gamma = 67°$.

The crystallization process affects polymer properties through the crystal structure and morphology established during the solidification process. An important aspect of the crystallization process is its kinetics, both from the fundamental view of polymer physics and for the modeling and control of polymer processing operations. In practical processing, such as extrusion molding and film forming, crystallization usually proceeds under isothermal and non-isothermal conditions. In order to obtain materials with better physical properties, it is important to study the isothermal and non-isothermal crystallization processes. The thermal properties, isothermal and non-isothermal crystallization kinetics of nylon 1212 were studied by differential scanning calorimeter (DSC) in this article.

---

* Corresponding author. Tel.: +86-371-776-3524; fax: +86-371-776-3524.
E-mail address: lmy@zzu.edu.cn (Q. Zhao).

0032-3861/03/$ - see front matter © 2003 Elsevier Science Ltd. All rights reserved.
doi:10.1016/S0032-3861(03)00101-0

2. Experimental

2.1. Materials and preparation

The sample of nylon 1212 was provided by Zibo Guangtong Chemical Co. Ltd (China) with a η_r of 1.76. The η_r was determined by viscosimetry in H_2SO_4 (96%) at 25 °C. The samples were kept in a vacuum oven at 80 °C for 8 h before use.

2.2. Differential scanning calorimetry

Isothermal and non-isothermal crystallization kinetics was carried out using a Perkin–Elmer DSC-7 differential scanning calorimeter calibrated the temperature with indium. All DSC were performed under nitrogen atmosphere; sample weights were between 5 and 8 mg.

2.3. Isothermal and non-isothermal crystallization process

The isothermal crystallization and melting process were performed as follows: the samples were heated quickly (at 80 °C/min) to 20–30 °C above the melting temperature (T_m), stayed there for 10 min to eliminate residual crystals, then cooled (at −80 °C/min) to the designated crystallization temperatures (T_c) in the range of 160–171 °C for the isothermal crystallization for 10 min, and then heated to 210 °C at a rate of 10 °C/min.

The non-isothermal crystallization was performed as follows: The samples were heated quickly (at 80 °C/min) to 20–30 °C above the melting temperature (T_m), stayed there for 10 min to eliminate residual crystals, then cooling the melt to crystallize at different cooling rates, 2.5, 5, 10, 20, 40 °C/min. The exothermic curves of heat flow as a function of time were recorded and investigated.

3. Results and discussion

3.1. Melting behavior and equilibrium melting temperature

Fig. 1 presents a serial of DSC heating thermograms of nylon 1212 samples that melt-crystallized at different T_c (160–171 °C). It is apparent that the DSC endotherms exhibit three melting peaks. Peak I is present in all samples at a temperature close to its crystallization temperature ($T \approx T_c + 4$ °C), and moves more sharply to higher temperatures than Peak II. Apparently, Peak I and peak II tend to combine together with crystallization temperature increasing. Peak III is situated at about 186 °C in all samples. According to similar explanations of multiple endotherms of nylon 6 [19], nylon 610 [20], These Peaks mainly refer to the melting of the crystals with different crystal perfection. The cause of peak I is assumed to be microcrystallite formation in the boundary layer between the larger crystallites, and Peak III corresponds to the melting of the furthest perfect crystals. From Fig.1, we can see that the area of Peak II is much larger than that of Peak I or Peak III, which indicates that Peak II is caused by the melting of the major crystal.

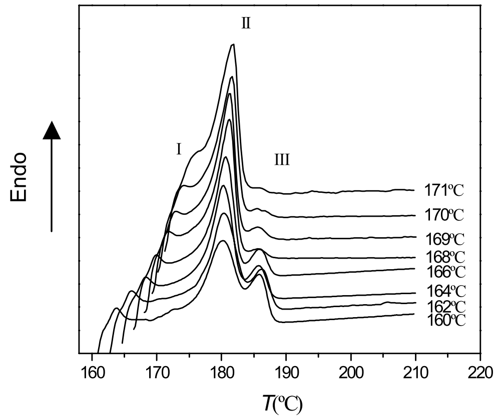

Fig. 1. Melting endotherms of nylon 1212, recorded at the heating rate of 10 °C/min, after isothermal crystallization at the specified temperature.

Fig. 2 shows the plot of T_m versus T_c. It is evident that T_m values exhibit a linear relationship with T_c. From both of Fig. 1 and Fig. 2, we can see that peak III remains almost constant and independent of T_c. Although T_m (I) varies linearly with T_c, it is parallel with the line $T_m = T_c$. Therefore, both peak I and III are useless in the determination of the equilibrium melting temperature T_m^0 of nylon 1212. Only T_m (II) varies linearly with T_c, and not parallel with the line $T_m = T_c$. According to a theory derived by Hoffman and Weeks [21], the equilibrium melting temperature T_m^0, that is the melting temperature of infinitely extended crystals, can be obtained by linear extrapolation of T_m (II) versus T_c data to the line $T_m = T_c$. Mathematically, they arrived at the following equation:

$$T_m = \frac{T_c}{2\beta} + T_m^0\left[1 - \frac{1}{2\beta}\right] \tag{1}$$

where β is the 'thickening ratio'. In other words, β indicates

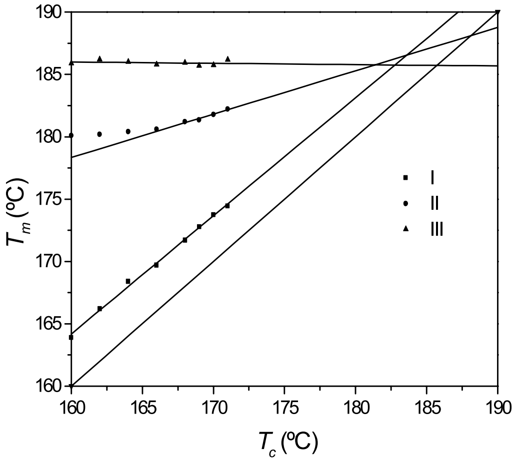

Fig. 2. Melting temperatures as a function of crystallization temperatures for the nylon 1212 samples.

the ratio of the thickness of the mature crystal L_c to that of the initial one L_c^*, ; therefore, $\beta = L_c/L_c^*$, which is supposed to always be greater than or equal to 1. It should be noted that the factor 2 in Eq. (1) suggests that the thickness of the crystals undergoing melting is approximately doubled that of the initial critical thickness. It well known that the higher the isothermal crystallization temperature it is more suitable to get the equilibrium melting temperature [20]. According to Fig. 2, the lower isothermal crystallization temperatures do not fit to calculate the equilibrium melting temperature, so we use the much higher isothermal crystallization temperature to calculate the equilibrium melting temperature. The T_m^0 of nylon 1212, 188.0 °C, was obtained by extrapolation of the T_m(II) versus T_c curve. For polyamides, there is a trend that the longer the hydrocarbon segment in the repeating unit, the lower the value of T_m^0. Therefore, the value of T_m^0 of nylon 1212 can be said to be reasonable compared with nylon 66 (280 °C) [19], nylon 610 (238 °C) [20] and nylon 1010 (214 °C)[22].

3.2. Isothermal crystallization kinetic analysis

3.2.1. Analysis based on the Avrami equation

In order to compare the results more apparently, we adopt the isothermal crystallization step of 2 °C from the beginning 160 °C to the end 170 °C. The crystallization process is usually treated as a composite of 2 stages: the primary crystallization stage and the secondary crystallization stage. The crystallization process is very marked in its temperature dependency. Assuming that the relative crystallinity increases with the crystallization time t increasing, then the Avrami equation [Eq. (2)] [23,24] can be used to analyze the isothermal crystallization process of nylon 1212, as follows:

$$X(t) = 1 - \exp(-Kt^n)$$
$$\lg[-\ln(1 - X(t))] = n\lg t + \lg K \qquad (2)$$

Where $X(t)$ is the weight fraction of crystallized material at time t, n is the Avrami exponent and K is the crystallization rate parameter. The double logarithmic plot of $\lg[-ln(1 - X(t))]$ versus $\lg t$ is shown in Fig. 3. We can see that each curves is composed of two linear section. This fact indicates the existence of a secondary crystallization of nylon 1212, with the deviation due to the secondary crystallization that is caused by the spherulite impingement in the later stage of crystallization process [24,25,26]. By performing a least square fit to the Avrami plots, the Avrami expoent n and the rate constant K can readily be extracted. The values of n and K are determined from the initial linear section and the results are shown in Table 1. From Table 1, it can be seen that the Avrami parameter n is range from 1.56 to 2.03, depending on the crystallization temperature T_c. These results indicate that the spherulites nucleate and grow freely at the primary crystallization stage; the crystallization mode of nylon 1212 might be the mixture with one-dimensional, needle-like and two-dimensional, circular, diffusion controlled growth with thermal nucleation. The values of the crystallization rate parameters K increase with the crystallization temperature T_c decreasing, and exhibit very different temperature dependency characteristic of nucleation-controlled and thermal-activated crystallization associated with the proximity to the melting temperature (T_m).

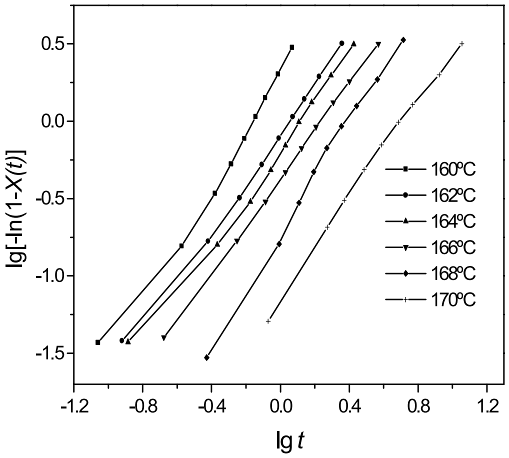

Fig. 3. Plot of $\lg[-\ln(1 - X(t))]$ versus $\lg t$ for isothermal crystallization at the indicated temperatures.

Fig. 4 shows the $X(t)$ values obtained as functions of crystallization time (t) for nylon 1212 at different temperatures. It can be seen from Fig. 4 that the characteristic sigmoidal isotherms are shifted to right along the time axis with the isothermal crystallization temperatures increasing, indicating progressively slower crystallization rate.

The another important parameter is the half-time of crystallization $t_{1/2}$ which is defined as the time taken from the onset of the crystallization until 50% completion and can be extracted directly from the plot of $X(t)$ versus t (Fig. 4). That is,

$$t_{1/2} = (\ln 2/K)^{1/n} \qquad (3)$$

The dependence of $t_{1/2}$ upon the crystallization temperature is shown in Fig. 5. As observed in all polymeric materials $t_{1/2}$ increases slowly with T_c increasing for lower supercooling degree.

Usually, the rate of crystallization G is described as the reciprocal of $t_{1/2}$; that is to say, $G = \tau_{1/2} = (t_{1/2})^{-1}$. The values of $\tau_{1/2}$ and $t_{1/2}$ are listed in Table 1. Lin [27] used Eq. (2) to calculate the necessary time for maximum crystallization rate, $t_{\max}$, since this time corresponds to the point

Table 1
Kinetic parameters for isothermal crystallization of nylon 1212

T_C (°C)	160	162	164	166	168	170
n	2.03	1.65	1.67	1.56	1.68	1.64
K (min^{-1})	2.12	0.81	0.62	0.42	0.22	0.08
$t_{\max}$ (min)	0.49	0.64	0.76	0.90	1.44	2.72
$t_{1/2}$(min)	0.58	0.91	1.06	1.37	1.99	3.86
$\tau_{1/2}$(min^{-1})	1.74	1.10	0.94	0.73	0.50	0.26

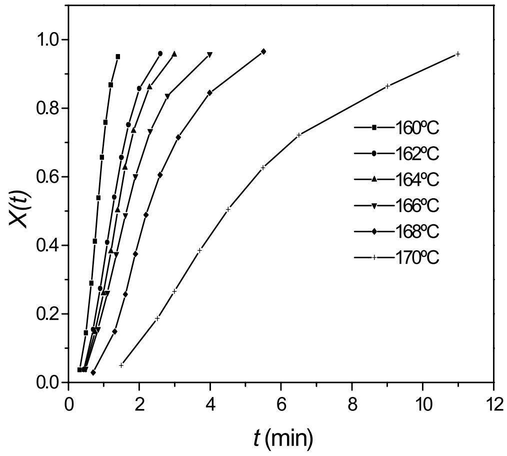

Fig. 4. Development of relative degree of crystallization $X(t)$ with time t for isothermal crystallization of nylon 1212 at different crystallization temperatures.

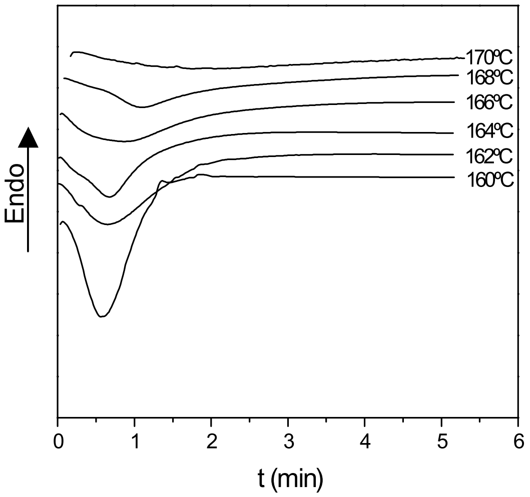

Fig. 6. Heat flow versus time during isothermal crystallization of nylon 1212 at the different crystallization temperatures by DSC.

where $dQ(t)/dt = 0, Q(t)$ is the heat-flow rate, obtaining

$$t_{\max} = [(n-1)/nK]^{1/n} \tag{4}$$

The calculated values of $t_{\max}$ are listed in Table 1. Data of $t_{\max}$ can also be obtained from the heat-flow curves in Fig. 6.

The cyclic diagram of thermal analysis for nylon 1212 in Fig. 6 is recorded by heating the amorphous film from room temperature to 20–30 °C above the melting temperature (T_m) at 10 °C/min, maintaining it for 10 min in order to remove all residues of crystallinity, and then cooling down (at −80 °C/min) to various crystallization temperatures, T_c. With the crystallization temperature increases, the crystallization exothermal peaks shifted to longer times and became flat (Fig.6); it implies that the total crystallization time is lengthened, and the crystallization rate decreases with the increased T_c (Table 1).

3.2.2. Crystallization activation energy (ΔE)

The crystallization process for bulk nylon1212 is assumed to be thermally activated, then the crystallization rate parameter K can be approximately described by the following Arrhenius equation [28]

$$\begin{aligned} K^{1/n} &= k_0 \exp(-\Delta E/RT_c) \\ (1/n)\ln K &= \ln k_0 - \Delta E/RT_c \end{aligned} \tag{5}$$

where k_0 is a temperature independent preexponential factor, R is the gas constant, and ΔE is the crystallization activation energy. ΔE can be determined by the slop coefficient of plots of $(1/n)\ln K$ versus $1/T_c$ (Fig. 7). The value of the activation energy for the primary crystallization process is found to be −284.5 KJ/mol. Because it has to release energy while transforming the molten fluid into the crystalline state, the value of ΔE is negative on the basis of the concept of heat quantity in physical chemistry.

From Turnbull–Fisher expression [Eq. (6)] [29]

$$\ln G = \ln G_0 - \frac{\Delta E^*}{kT_c} - \frac{\Delta F^*}{kT_c} \tag{6}$$

where G is the spherulitic growth rate, G_0 is a preexponential factor, k is Boltzmann constant, T_c is the crystallization temperature, ΔE^* is the free energy of activation for

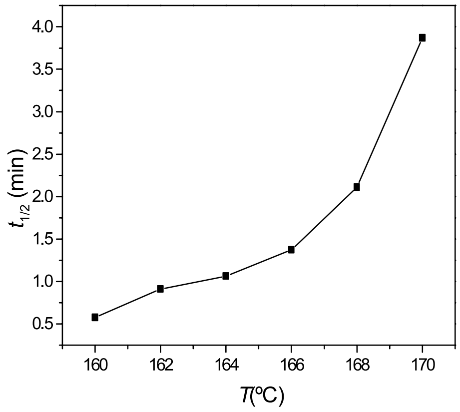

Fig. 5. the $t_{1/2}$ versus T_c of isothermal crystallization for nylon 1212.

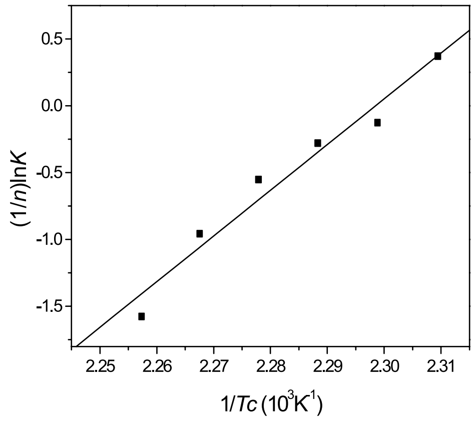

Fig. 7. $(1/n)\ln K$ versus $1/T_c$ for Avrami parameter K deduced from isothermal crystallization.

transporting a chain segment from the supercooled to the crystalline phase, and ΔE^* is the free energy of formation of a nucleus of critical size. At low temperature, the transportation term, $-\Delta E^*/kT_c$, decreased rapidly; when T_c is approached to T_g, the transportation term should be dominant for the crystallization rate. At high temperature (that is, the melt crystallization T_c approached T_m), the nucleation term, $-\Delta F^*/kT_c$, decreased rapidly, and it should be dominant for the crystallization rate in the melt crystallization process; the result can be explained as the presence of a maximum in the behavior of the growth rate [30,31]. In our experiment, the values of T_c are 160–170 °C, which approached $T_m = 183$ °C, so $\Delta E_*/kT_c$ is negligible in the isothermal crystallization process for nylon 1212. This lead to

$$\ln G = \ln G_0 - \Delta F^*/kT_c$$
$$\ln G = \ln G_0 - \frac{\chi T_m^0}{T_c^2(T_m^0 - T)_c} \tag{7}$$

where G, the crystallization rate, is controlled by a single nucleation term and the term for $\Delta F^*/kT_c$ is adapted as derived by Hoffmann, T_m^0 is the equilibrium melting point ($T_m^0 = 188.0$ °C) and X is a parameter concerned with the heat of fusion and the interfacial free energy.

From Eqs. (2), (4) and (7), Lin [27] obtained

$$\lg t_{max} = B - \frac{C}{2.303 * T_c^2 * \Delta T} \tag{8}$$

where B and C are constants, and ΔT is the degree of supercooling ($\Delta T = T_m^0 - T_c$). Eq. (8) can be used to verify the possibility that nylon 1212 could be described by Avrami equation at the primary stage of the isothermal crystallization. This means that drawing a plot of $\lg t_{max}$ versus $1/(T_c^2\Delta T)$, if the plot is a straight line, it is very like that nylon 1212 can be described as undergoing primary crystallization at t_{max}. The plot is shown in Fig. 8, and it has a good linear relation.

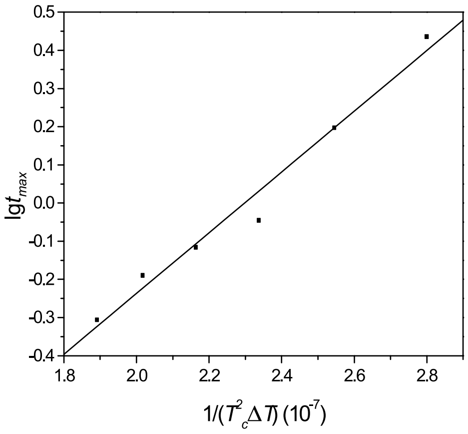

Fig. 8. Plot of $\lg t_{max}$ versus $1/(T_c^2\Delta T)$ of nylon 1212.

3.3. Non-isothermal crystallization kinetic analysis

3.3.1. Avarmi equation by Jeziorny modified

The non-isothermal crystallization exothermic peaks of nylon 1212 at various cooling rates, Φ, are shown in Fig. 9. T^* is the peak temperature where the crystallization rate is maximum, and T^* moves to a low temperature region with increasing the cooling rate.

From the DSC digital information, we calculate the values of relative crystallinity $X(t)$ at different crystallization temperatures T, shown in Fig. 10(a). We obtained a series of reversed S-shaped curves. A relationship between crystallization temperature T and time t is given by Eq. (9) during the non-isothermal crystallization process, as follows:

$$t = \frac{|T_0 - T|}{\Phi} \tag{9}$$

where T_0 is the initial temperature when crystallization begins ($t = 0$). The values of X-axis in Fig. 10 (a) could be transformed into crystallization time t [shown in Fig. 10(b)]. Because of the spherulite impingement in the later stage, the curves tend to flat and became S-shaped (or reversed S-shaped). We can obtain the values of T or t at the various cooling rates from Fig. 10 at a random relative crystallinity $X(t)$. Through Fig. 10(b), we can get the half time of non-isothermal crystallization, $t_{1/2}$, when the $X(t)$ are equal to 50%. The peak temperature T^*, the half-time of crystallization $t_{1/2}$ and the crystallization enthalpies ΔH_c at different cooling rates are listed in Table 2. The data indicate that for the T^*, very different rate dependencies exist in the melt crystallization for nylon 1212. And the $t_{1/2}$ indicates that the higher the cooling rate, the shorter the time of crystallization completion.

Mandelkern [32] considered that the primary stage of non-isothermal crystallization can be described by the Avrami equation, based on the assumption that the crystallization temperature is constant. Mandelkern obtained the

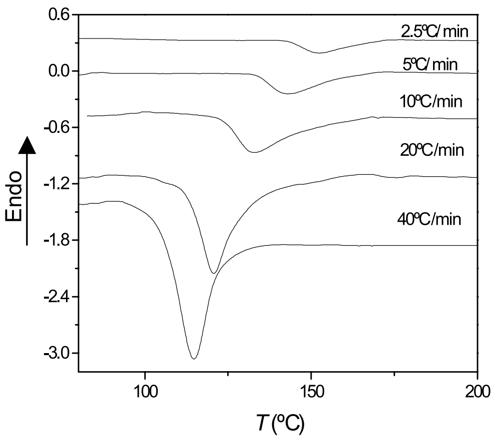

Fig. 9. Heat flow versus temperature during non-isothermal crystallization of nylon 1212 at different cooling rates by DSC.

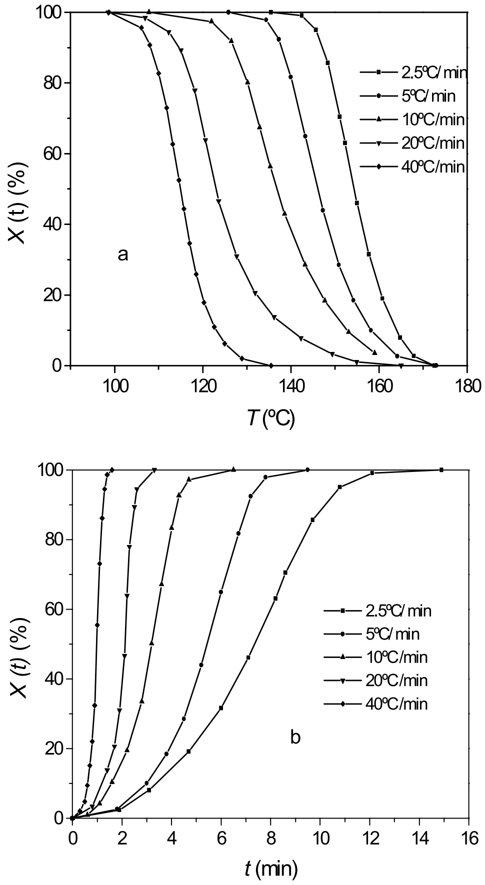

Fig. 10. (a) Relative crystallinity $X(t)$: at different crystallization temperatures T and (b) at different crystallization times t in the process of non-isothermal crystallization for nylon 1212.

following:

$$\begin{aligned} &1 - X(t) = \exp[-Z_t t^n] \\ &\lg\{-\ln[1 - X(t)]\} = n \lg t + \lg Z_t \end{aligned} \tag{10}$$

where Z_t is the rate constant in the non-isothermal crystallization process. Jeziorny [33] considered the values of Z_t determined by Avrami Eq. (10) should be adequate. Considered to be an influence on the cooling or heating rate $\Phi = \mathrm{d}T/\mathrm{d}t$, Jeziorny assumed that Φ was constant or approximately constant. The final form of the rate parameter characterizing the kinetics of non-isothermal crystallization is given as follows:

$$\lg Z_c = \frac{\lg Z_t}{\Phi} \tag{11}$$

Table 2
The values of T^*, $t_{1/2}$ and ΔH_c in non-isothermal crystallization for nylon 1212

Φ (K/min)	2.5	5	10	20	40
T^*(°C)	152.4	143.3	133.1	120.7	114.6
$t_{1/2}$ (min)	7.7	5.9	3.3	2.5	1.6
ΔH_c (J/g)	51.24	48.28	50.94	50.52	46.56

Drawing the straight line corresponding to $\lg[-\ln(1 - X(t))]$ versus $\lg t$ by using Eq. (10), we can determine the values of Avrami exponent n and the rate parameter Z_t or Z_c from the slope and intercept (Fig. 11). The values of n, Z_t, Z_c, and $\tau_{1/2}$ are shown in Table 3. Like the Process of isothermal crystallization (Fig. 3), all curves are divided into the following 2 sections the primary crystallization stage, and the secondary crystallization stage. At the secondary stage, the straight line tends to deviate primary crystallization stage. The result also indicates the existence of a secondary crystallization in the process of non-isothermal crystallization for nylon 1212. At the primary stage, the Avrami exponent, n_1 in the range of 2.38–3.05, indicates that the mode of the nucleation and growth at primary stage of the non-isothermal crystallization for nylon 1212 may be two-dimensional, three-dimensional space extension, circular, diffusion controlled growth with thermal nucleation and the crystallization more complicated than those of the isothermal crystallization process. At the secondary stage, the Avrami exponent, $n_2 \geq 4$ (Table 3), because of the spherulites' impingement and crowding, and the growth form of spherulites mode becomes more complicated than those of the primary stage process.

3.3.2. Average Avrami parameter

A new method was reported to determine the average Avrami exponent [34] $\bar{n}$ from experimental crystallization exotherms with peak maximum (T^*) and two inflexion points (T_1, T_2) for different cooling rates. Firstly, in determination of $\bar{n}$ at a constant cooling rate, the following equation proposed by Ozawa [35] is used:

$$[X_v(T)]_\Phi = 1 - \exp\left(-\frac{K(T)}{\Phi^n}\right) \tag{12}$$

where $X_v(T)$ is the volume fraction of transformed polymer at a temperature T, Φ is the cooling rate, and $K(T)$ is the so-called cooling function. Assuming linear dependence between $\ln K(T)$ versus temperature as suggested by the

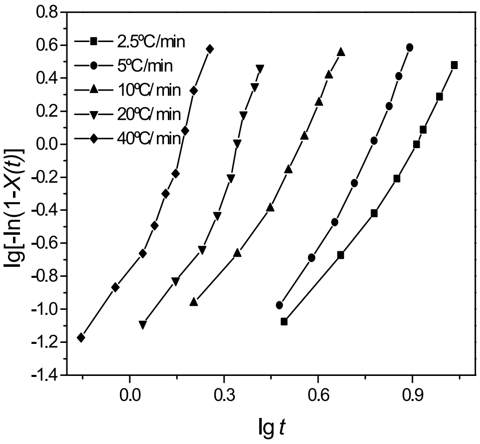

Fig. 11. Plots of $\lg[-\ln(1 - X(t))]$ versus $\lg t$ for non-isothermal crystallization process of nylon 1212.

Table 3
The values of n, Z_t, Z_c and $\tau_{1/2}$ from the Avrami equation at the two of non-isothermal crystallization for nylon 1212

Φ (K/min)	Primary crystallization stage				Secondary crystallization stage			
	n_1	Z_{t1}	Z_{c1}	$\tau_{1/2}$ (min^{-1})	n_2	Z_{t2}	Z_{c2}	$\tau_{1/2}$ (min^{-1})
2.5	2.38	5.53×10^{-3}	0.125	0.13	3.99	2.29×10^{-4}	0.035	0.13
5	3.05	3.56×10^{-3}	0.324	0.17	4.99	1.33×10^{-4}	0.168	0.18
10	2.61	3.01×10^{-2}	0.704	0.30	4.44	3.81×10^{-3}	0.573	0.31
20	2.67	6.14×10^{-2}	0.870	0.40	5.95	9.81×10^{-3}	0.794	0.48
40	2.80	1.81×10^{-1}	0.958	0.62	6.08	1.10×10^{-1}	0.946	0.74

theory:

$$\ln K(T) = aT + b \qquad \Rightarrow \qquad K(T) = \exp(aT + b) \tag{13}$$

So, T^*, T_1 and T_2 as a function of $\ln\Phi$ can be expressed as:

$$T^* = \frac{\bar{n}}{a}\ln\Phi - \frac{b}{a} \tag{14}$$

$$T_1 = \frac{\bar{n}}{a}\ln\Phi + \frac{\ln\left(\frac{3-\sqrt{5}}{2}\right)}{a} - \frac{b}{a} \tag{15}$$

$$T_2 = \frac{\bar{n}}{a}\ln\Phi + \frac{\ln\left(\frac{3+\sqrt{5}}{2}\right)}{a} - \frac{b}{a} \tag{16}$$

From the different crystallization peaks for cooling rates between 2.5 and 40 K/min, the values of the temperature T_1 (first inflexion point), T^* (maximum of the peak), and T_2 (second inflexion point) were determined. According to the theory, these temperatures vary linearly with the cooling rate logarithm (Fig. 12). It was established that under these conditions the three lines are parallel to each other, and the slopes of the three straight lines are identical for the setting cooling rates. Therefore, in a general manner, T_1, T^*, and T_2 may be expressed as $T_i = A\ln\Phi + B_i$. So, the following simple system was resolved:

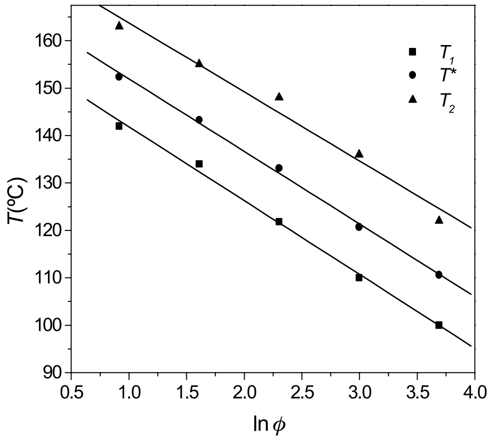

Fig. 12. The plots of evolution of T_1, T^*, and T_2 of nylon 1212 as a function of $\ln\Phi$.

$$\frac{\bar{n}}{a} = A, \qquad \frac{\ln\left(\frac{3-\sqrt{5}}{2}\right)}{a} - \frac{b}{a} = B_1 \qquad \Rightarrow$$

$$\bar{n} = A \times \frac{\ln\left(\frac{3-\sqrt{5}}{3+\sqrt{5}}\right)}{B_1 - B_2}, \tag{17}$$

$$\frac{\ln\left(\frac{3+\sqrt{5}}{2}\right)}{a} - \frac{b}{a} = B_2$$

From the experimental results presented in Fig. 12, the coefficients A, B_1, and B_2 are, respectively, calculated to be:

$A = -15.58$; $B_1 = 172.74$; $B_2 = 157.44$

Under these conditions, $\bar{n} = 1.96$.

3.3.3. Combined Avrami equation and Ozawa equation

It is evident that the Avrami analysis and its Jeziorny modification could describe only the primary stage of non-isothermal melt crystallization of nylon 1212. In order to find a method to describe exactly the non-isothermal crystallization process, Mo et al., adopted a novel kinetic approach by combining the Avrami equation with the Ozawa equation [35] and successfully dealt with the non-isothermal crystallization behavior of nylon 11 [36], PEDEKK [37], polyalkylthiophenes [38] and nylon 66 [39]:

$$\lg Z_t + n\lg t = \lg K(T) - m\lg\Phi,$$

$$\lg\Phi = \frac{1}{m}\lg\left[\frac{K(T)}{Z_t}\right] - \frac{n}{m}\lg t$$

Its final form is:

$$\lg\Phi = \lg F(T) - a\lg t \tag{18}$$

where $F(T) = [K(T)/Z_t]^{1/m}$, and $a = n/m$; the parameter $F(T)$ is the value of cooling rate, which has to be chosen at unit crystallization time when the measured system amounts to a certain degree of crystallinity. It could be seen that $F(T)$ had a definite physical and practical meaning. At a given degree of crystallinity, the plots of $\lg\Phi$–$\lg t$ are given in Fig. 13, from which the values of $F(T)$ systematically

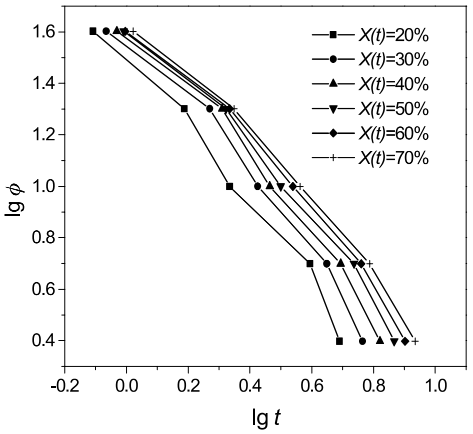

Fig. 13. The plots of lg ø versus lg t from the combined Avrami and Ozawa equation for nylon 1212.

increase with rising relative crystallinity, indicating that at unit crystallization time, a higher cooling rate should be used in order to obtain a higher degree of crystallinity; nevertheless, the values of a are almost constant.

3.3.4. Crystallization activation energy (ΔE)

Considering the influence of the various cooling rate Φ in the non-isothermal crystallization process, Kissinger [40] reported that the activation energy ΔE could be determined by:

$$\frac{\mathrm{d}[\ln(\Phi/T^{*2})]}{\mathrm{d}(1/T^{*})} = -\frac{\Delta E}{R} \tag{19}$$

where R is the gas constant and T^{*} is the peak temperature. The good linear relation plot of $\lg(\phi/T^{*2})$ versus $1/T^{*}$ is shown in Fig. 14. The slope $= \mathrm{d}[\lg(\phi/T^{*2})]/\mathrm{d}1/T^{*} = -\Delta E/2.303R$, and $\Delta E = -102.63$ KJ/mol for nylon 1212.

4. Conclusion

Observation of subsequent melting of nylon 1212 samples after isothermal crystallization at specified crystallization temperatures showed the existence of three endotherms whose position on the temperature axis and heat absorbed depended significantly on the crystallization temperature. Peak I is microcrystallite formation in the boundary layer between the larger crystallites. Peak II is the major crystal in the isothermal crystallization process, whereas peak III remains almost constant and independent of T_c. The typical Hoffman-Weeks extrapolation suggested that the equilibrium melting temperature T_m^0 is 188.0 °C. The Avrami analysis indicates that the crystallization process is composed of the primary stage and the secondary stage. At the primary stage, the Avrami exponent $n = 1.5-2.0$ in nylon 1212, and the process of crystal nucleation and growth is a mixture of a one-dimensional, needle-like process and a two-dimensional, circular, diffusion-controlled process.

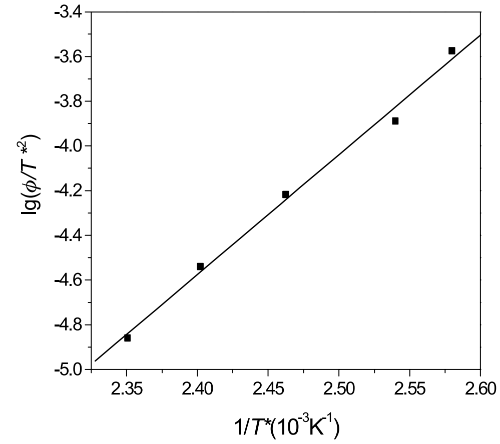

Fig. 14. The plot of $\lg(\Phi/T^{*2})$ versus $1/T^{*}$ from the Kissinger method for nylon 1212.

At the primary stage in the non-isothermal crystallization process, the Avrami exponent, n_1 in the range of 2.3–3.0, indicates that the process of crystallization is two-dimensional, three-dimensional space extension, circular, diffusion controlled growth with thermal nucleation and the crystallization more complicated than those of the isothermal crystallization process. The $\bar{n}$ is 1.96. With Mo's method, we successfully describe the non-isothermal crystallization process.

Acknowledgements

The authors are grateful to Prof. Lixia Li and Yuchen Qi of State Key Laboratory of Polymer Physics & Chemistry, Changchun Institute of Applied Chemistry of China for the DSC measurements. The work reported herein was supported by Natural Science Foundation of Henan Province (974002600)

References

[1] Welgos RJ, Encyclopedia of Polymer science and Engineering, vol. 2. New York: Wiley; 1988. p. 11.

[2] Kohan MI. Nylon Plastics Handbook. Munich: Carl Hanser Verlag; 1995. Chapter 10.

[3] Carothers WH. US Patent 1938; 2 130 948.

[4] Carothers WH, Graves GD. US Patent, 1939; 2 163 584.

[5] Nieschlag HJ, Wolff IA. J Am Oil Chem Soc 1971;48:723.

[6] Anon Japanese Patent 1989; 1 306 417 (Mitsui Toatsu Chem., Inc.).

[7] Liu CK, Kokish M. Polym Prepr 1996;37(1):748.

[8] Mark HF, Atlas SM. Chem Eng 1961;11:143ff.

[9] Shi YB, Groleau MR, Yee AF, Wiley PC, Yang HJ, Bertram JL. Proc ACS Div Polym Mater Sci Eng 1994;70:110.

[10] Pathmanathan K, Johari GP. J Polym Sci Part B (Polym Phys) 1993; 31:265.

[11] Del Nobile MA, Mensitieri G, Lostocco LR, Huang SJ, Nicolais L. Packaging Technol Sci 1997;10:311.

[12] Sims WM, Bliss AD. German Patent 1972; 2 225 515.

[13] Sims WM. German Patent 1976; 2 626 273.

[14] Jones NA, Atkins EDT, Hill MJ, Cooper SJ, Franco L. Polymer 1997;38:2689.
[15] Wang LH, Balta Calleja FJ, Tetsuo K, Roger SP. Polymer 1993;34:4688.
[16] Ehrenstein M, Dellsperger S, Kocher C, Stutzmann N, Weder C, Smith P. Polymer 2000;41:3531.
[17] Jones NA, Atkins EDT, Hill MJ. J Polym Sci Part B (Polym Phys) 2000;38:1209.
[18] Jones NA, Atkins EDT, Hill MJ. Macromolecules 2000;33:2642.
[19] Wunderlich B. Macromolecular Physics. Crystal Melting, vol. 3. New York: Academic Press; 1980.
[20] Wang GM, Yan DY, Bu HS. Chin J Polym Sci 1998;16:243.
[21] Hoffman JD, Weeks JJ. J Res Natl Bur Stand 1962;A66:13.
[22] Mo ZS, Meng QB, Feng JH. Polym Int 1993;32:53.
[23] Avarami M. J Chem Phys 1939;7:1103.
[24] Avarami M. J Chem Phys 1940;8:212.
[25] Wunderlich B, Macromolecular Physics, vol. 2. New York: Academic Press; 1977.
[26] Liu JP, Mo ZS. Chin Polym Bull 1991;4:199.
[27] Lin CC. Polym Eng Sci 1983;23:113.
[28] Cebe P, Hong SD. Polymer 1986;27:1183.
[29] Turbull D, Fisher JC. J Chem Phys 1949;17:71.
[30] Ziabicki A. Appl Polym Symp 1967;6:1.
[31] Baer E, Collier JR, Carter DR. SPE Trans 1965;5:22.
[32] Fava RA. Methods of Experimental Physics. Polymers, Part B: Crystal Structure and Morphology, vol. 16B. New York: Academic Press, Inc; 1980.
[33] Jeziorny A. Polymer 1978;19:1142.
[34] Cazé C, Devaux E, Crespy A, Cavrot JP. Polymer 1997;38:497.
[35] Ozawa T. Polymer 1971;12:150.
[36] Liu SY, Yu YN, Cui Y, Zhang HF, Mo ZS. J Appl Polym Sci 1998;70:2371.
[37] Liu TX, Mo ZS, Zhang HF. J Polym Eng 1998;18(4):283.
[38] Qiao XY, Sun ZC, Zhao XJ, Wang XH, Zhang HF, Mo ZS. Acta Polym Sinica 1999;6:649.
[39] Zhang QX, Mo ZS. Chin J Polym Sci 2001;19:237.
[40] Kissinger HE. J Res Natl Stand (US) 1956;57:217.